海洋湖沼通报
1994年 Transactions of Oceanology and Limnology No. 2

DEVELOPMENT OF EL NINOS DURING 1971—1992

Wang Bin and Wang Yan
(Department of Meteorology, School of Ocean and Earth Science and Technology, University of Hawaii)

Abstract

The El Nino-Southern Oscillation (ENSO) cycle is demonstrated to be highly variable. The dominant frequency changes with time, resulting in a broad band of period ranging from 2 to 7 years. In the mid-1960s the dominant period changed suddenly from 6 years to about 2 years. From the mid-1960s to mid 1970s the period increased gradually from 2 years to 4 years. After the mid-1970s the ENSO cycle has been a quasi 5 year oscillation with a significant quasi-biennial component, and the ENSO events bear considerable similarities in their transition from a cold to a warm state.

Multi-variate empirical orthogonal function (MV-EOF) analysis of the post-1970 data indicates that the most significant mode describes the mature phase of ENSO, and the second most significant mode describes an early stage in the ENSO warming. The development of a warm episode is characterized by (a) a planetary-scale low pressure anomaly in the tropical North Pacific, (b) an accompanying quasi-geostrophic cyclonic gyre with relatively strong westerly anomalies in the western equatorial Pacific and enhanced trades in the eastern equatorial Pacific, (c) a convection anomaly overlapping with the westerly anomaly over the western Pacific due primarily to the meridional wind convergence. This mode displays a significant quasi-biennial component, in contrast to the frist EOF mode which depicts the mature phase of El Nino and exhibits a dominant 5-year period.

Key words: El Nino-Southern Oscillation (ENSO), Multi-variate empirical orthogonal function (MV-EOF).

本文1993年12月18日收到

1. Introduction

The anomalous warming of the tropical eastern-central Pacific Ocean and along the South American coast (termed as El Nino hereafter) occurs in tandem with the weakening of the southeast trades, which is in turn tied to the simultaneous pressure fall in the southeast Pacific and pressure rise over Indonesia (a low-index phase of the Southern Oscillation). This coupled variation of the ocean and atmosphere climate system is referred to as El Nino-Southern Oscillation(ENSO).

The alternative occurrences of El Nino and La Nina (Philander 1985) and the low-and high-index states of the Southern Oscillation (SO) are now popularly viewed as a cycle---the ENSO cycle. The ENSO cycle exhibits a broad band of period ranging from 2 to 7 years. In section 3 we will demonstrate that this broad-band phenomenon is a result of the coexistence of multi-time scales and the temporal variation of the dominant frequency. We will also show that the frequency of ENSO has been steady after the 1970s with a dominant period of 4-5 years.

In one of his pioneering studies, Bjerknes (1969) raised a fundamental question regarding the nature of the ENSO cycle: How does the turnabout from a cold warm state take place? After a considerable number of studies in the last two decades (e.g., Wyrtki 1975, Barnett 1981, 1984, Rasmusson and Carpenter 1982, van Loon and Shea 1985, 1987, Trenberth and Shea 1987, Meehl 1987), this still remains an outstanding issue (Trenberth 1992, Cane 1993). Because of the cyclic and coupled nature of ENSO, it is difficult to search for any "initial" changes that may predict an El Nino.

One of the most influential observational studies to date is the work of Rasmusson and Carpenter (1982). They made a comprehensive description of a composite ENSO scenario based on the events during 1950-1976. Due to the poverty of data in the 1950s and the limited quality of the existing ship data, the Rasmusson-Carpenter (RC) composite El Nino basically consists of the three most significant events before 1976, i.e., the events of 1957, 1965, and 1972. The recent three events (1982, 1986-87, and 1991)displayed quite different behavior which was documented by Gill and Rasmusson (1983) for the 1982 event, Kousky and Leetmaa (1989) for the 1986-87 event, and Kousky (1993) and Janowiak (1993) for the 1991 event. A remarkable interdecadal change in the transition from a cold to a warm state of the ENSO cycle occurred in the late 1970s (Wang 1994a). The recent three ENSO events evolved from a similar background provided by a warm state of the latest interdecadal variation. They also occurred with a relatively steady phase of a quasi-five year periodic cycle. The latest three events, therefore,

share many common features.

In a previous study (Wang 1992), the vertical structure and development of the ENSO mode during 1979-1989 were studied in the equatorial zonal plane. The present analysis will extend that analysis to three dimensions and for an extended period from 1971-1992. The purpose of the present study is to investigate the development characteristics and the evolution of the three-dimensional structure of the coupled ENSO mode during the El Nino.

Section 2 discusses the data used in this study. Section 3 presents a wavelet analysis of the SST at the central equatorial Pacific which reveals the multi-time scale and nonstationary nature of the ENSO cycle. In section 4, multi-variable empirical orthogonal function (MV-EOF) analysis is used to reveal the spatial and temporal behavior of the ENSO mode in roughly the last two decades. The last section summarizes the results and discusses issues that call for future studies.

2. Data

The data used in the present study include Outgoing Longwave Radiation (OLR) data (July 1974-December 1992 with a nine-month gap in 1978), Highly Reflective Cloud (HRC) data from January 1971 to July 1985, and monthly mean SST, SLP, and surface winds from Comprehensive Ocean-Atmosphere Data Sets (COADS) for the period 1971-1992.

The OLR and HRC data are used as proxies to tropical deep convection. Their relations with precipitation are discussed in Wang (1994a). The original OLR data are on 2.5°x 2.5° grid and are obtained from the Climate Analysis Center/ National Meteorological Center. Their production and organization, e.g., the treatment of the inhomogeneities arsing from the differences in satellites and equatorial crossing times, were documented by Gruber and Krueger (1984). The HRC data were created by Garcia (1985) by subjective analysis of daily visible and infrared polar-orbiting satellite mosaics. The original data have a resolution of 1° × 1° for the global tropics between 25°S and 25°N. They describe deep, organized convective systems (cloud clusters) which are responsible for most tropical rainfall.

For the purpose of describing large-scale features, both OLR and HRC data were calculated with a coarser resolution of 5° x 5°. Regression equations for each grid between OLR and HRC were then derived using the data in the common periods from July 1974 to June 1987 with a nine-month gap in 1978 (147 months). The correlation coefficients are normally between -0.7 and-0.9 (Fig.1). The correlation is low in the southeast and northeast cold oceanic regions because the

OLR data were contaminated by stratocumulus and cirrus clouds. Using these regression equations, the monthly mean OLR from January 1971 to June 1974 and from April 1978 to December 1978 were estimated from observed HRC data. In this way, a continuous OLR data set was reconstructed for the period January 1971 to December 1992. It was used as a measure of convection and rainfall.

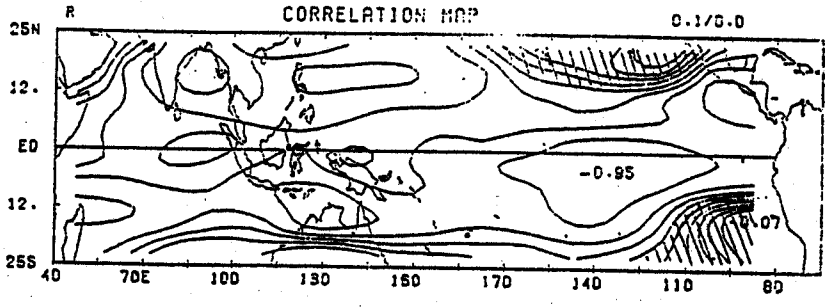

Fig. 1 Simultaneous correlation coefficient map between monthly mean outgoing longwave radiation (OLR) and highly reflective cloud (HRC) at 5°x5° grid. The sample size is 147. The contour interval is 0.1. Areas where the absolute value is less than 0.6 is shaded.

The original COADS data were on a 2° latitude by 2° longitude grid. To make a more reliable estimation of monthly means, the 2° x 2° data were combined into 5° (lat.) x 15° (long.) data by making observation-number-weighted box averages. For the purpose of describing the planetary-scale ENSO anomalies, this resolution is adequate. The averaged monthly observations in all the boxes for the period from January 1971 to December 1992 exceed 30. The averaged COADS were further carefully checked based on temporal and spatial consistency principles. For the details of the quality control refer to Wang (1994b).

The analysis domain covers the entire tropical Indian and Pacific Oceans between 25°S and 25°N and from 40°E to 80°W. All data were made for each 5° latitude by 15° longitude boxes (Total of 150 boxes). The variables analyzed in this study include SST, SLP, surface zonal and meridional winds, and OLR.

3. The nonstationary nature of the ENSO cycle

The SST at the central equatorial Pacific (170°W-155°W) (Fig. 2a) is qualified as an index for Pacific warming and used as an El Nino index in this paper for several resounding reasons. First, this box is located at the central Pacific ship tracks and has the best data density in the vast area of the equatorial Pacific from 160°E to 110°W. Second, the interannual variation of SST in this location

dominates the annual cycle: The annual cycle carries less than 10%, while the ENSO variation carries over 80% of the total variance. Third, the central Pacific warming signifies the mature phase of the El Nino (Rasmusson and Carpenter 1982) and has the most significant influence to the midlatitude circulation via teleconnections (Bjerknes 1966, Horel and Wallace 1980, Wallace and Gutzler 1981). Last and most important, the SST anomaly in this box can represent anomalous warming in the entire central and eastern equatorial Pacific from 170°W to 95°W. It also negatively correlated with the SO index (defined by the monthly mean pressure difference between Darwin and Tahiti) extremely well (Fig. 2b).

The El Nino index exhibits multi-time scales and variability (Fig. 3a). A

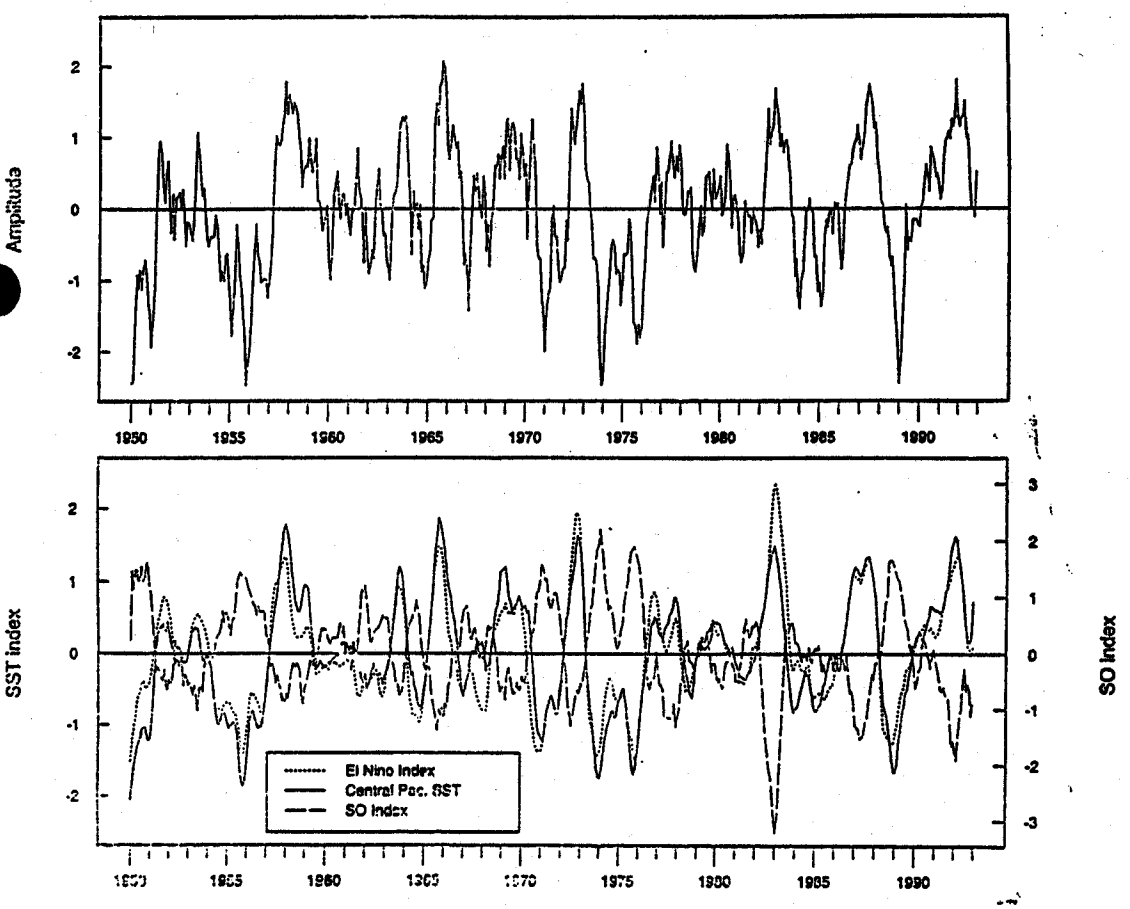

Fig. 2 (a) The monthly mean SST (the annual mean 27.8°C has been removed) at the central equatorial Pacific (5°S—5°N, 170°W—155°W); (b) Five—month running means of the SST anomalies at the central equatorial Pacific (5°S—5°N, 170°W—155°W) (solid) and in the eastern —central equatorial Pacific (5°S—5°N, 95°W—170°W) (dotted) and the Southern Oscillation index defined by the difference in monthly mean SLP between Darwin and Tahiti (dashed).

traditional Fourier analysis of time series gives a time-mean spectrum of the variability as a function of frequency without providing any temporal locality of the variation. It is, therefore, inadequate for the analysis of non-stationary time series.

A new technique, known as wavelet transform (WT), which was first introduced in seismic signal analysis (Morlet 1983, Goupillaud et al. 1984) and rapidly developed and applied to a broad range of phenomena such as turbulence (Farge 1992), has been recently adopted in Meteorology and Oceanography (e.g., Meyer et al. 1993, Weng and Lau 1993) for the analysis of non-stationary time series. A commonly-used continuous WT is Morlet WT. The detailed description of Morlet WT is not intended here. Only a very brief description is given below to facilitate those readers who are not familiar with WT.

Analogous to the Fourier transform, the Morlet WT of a signal f(t) is defined by the convolution (inner product) of the signal and a family of base functions (the Morlet wavelets) $M_{a;b}(t)$, i.e.,

$$W_M f(a,b) = \langle f(t), M_{a;b}(t) \rangle. \tag{1}$$

The Morlet wavelets, $M_{a;b}(t)$, are generated from a mother function M(t):

$$M_{a;b}(t) = a^{-1/2} M\left(\frac{t-b}{a}\right), \tag{2}$$

where

$$M(t) = \exp(iNt)\exp(-t^2/2) \tag{3}$$

represents an oscillation with a frequency N trapped in the vicinity of $t=0$. By introducing the parameters a and b into the mother wavelet (3), the Morlet wavelets (2) are able to change their frequency freely by varying parameter a and locate anywhere in the time domain by varying parameter b. The positive real parameter a is called dilation parameter, and the real parameter b is called translation parameter. The Morlet wavelet is thus acting as a flexible time-frequency window, which can automatically adjust its width and shift its center along the time axis, to detect local characteristics of the signal f(t).

The modulus of the complex $W_M f(a,b)$ can be interpreted as a measure of the energy density or variability of the signal f(t) at the time b and frequency 1/a. The real part of the Morlet WT of a signal combines the information of both modulus and phase and depicts the variability of the signal as a function of both time (b) and frequency (1/a). Oscillations that have significant energy only in some segments of time series may not be detected by Fourier transform, yet can be revealed by wavelet transform.

The maximum modulus of the Morlet WT of the Central Pacific SST (Fig. 3a) indicates the variation of the dominant frequency with time. Before 1964, the SST

variation had a primary period of six years, In the mid-1960s the dominant period suddenly changed to about 2 years. From the mid-1960s to mid-1970s, the period of the ENSO cycle increased gradually from about 2 years to 4 years. Since the mid-1970s, the ENSO cycle has been characterized by a steady quasi-5-year oscillation. This indicates that the ENSO cycle is highly nonstationary, and, its frequency has remarkable interdecadal variations.

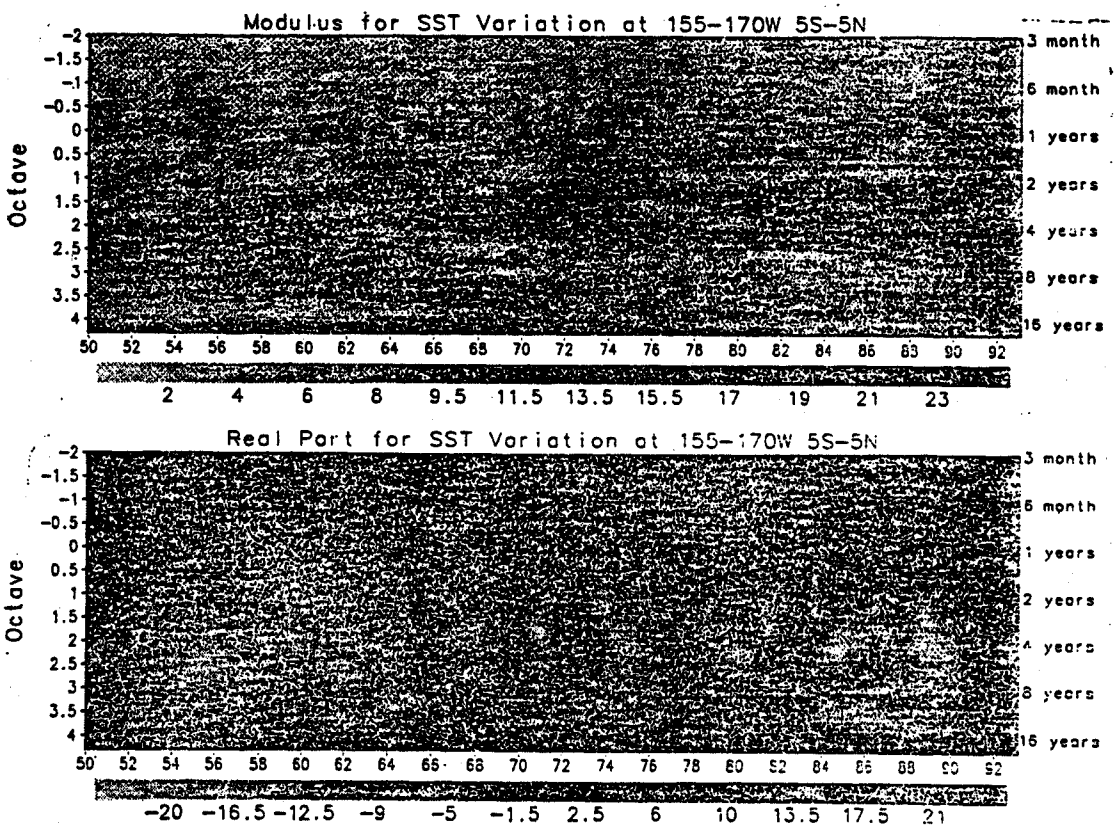

Fig. 3 (a) The modulus and (b) the real part of the Morlet wavelet transform of the central Pacific SST as a function of period and time. Note the change of the dominant frequency with time as depicted by the maximum modulus.

Figure 3a also indicates that in the central equatorial Pacific the annual cycle is much weaker than the interannual variation. Its amplitude is regulated by the interannual variation. During the years of strong or moderate La Ninas (1950, 1956, 1962. 1967. 1971. 1974. 1984. and 1989). the annual cycle is amplified as signified by the increase of the modulus. The quasi-biennial variation also has considerable low-frequency modulation on a decadal time scale and appears to be active in the period after 1970. The analysis in the following section will focus on

the last two decades in which the period of ENSO is relatively steady (a dominant 4-5 year mode with a minor quasi-biennial mode).

The real part of the Morlet WT of the Central Pacific SST (Fig. 3b) gives a instantaneous (local) spectral view of the ENSO cycle. The ENSO cycle can be viewed as a sum of the oscillations with different periods and amplitudes. The zero contours represent constant phase lines. A convergent pattern of the constant phase lines towards higher frequency depicts a singularity, or an extremely warm and cold event in the present case. The three strongest coolings in 1956, 1974, and 1989, and five most significant warmings in 1957-58. 1965, 1972, 1982, and 1987, all appear as a convergence of constant phase lines. The convergence can occur in different frequency bands, and represents in-phase reinforcement of two or three oscillation modes with different frequencies (e.g., quasi-biennial, four -year, six-year, and even decadal time scales).

4. Multivariate EOF analysis

To further reveal coherent variations in the coupled ocean-atmosphere climate system, we performed a five-variable (SST, SLP, surface zonal and meridional winds, and OLR) combined EOF analysis. The multi-variate EOF (MV-EOF) analysis, by making use of the property of both the spatial correlation and the correlation between geophysical fields, may extract dominant patterns of the spatial phase relationship among various fields of the derived EOFs. This often leads to useful physical insights into interactive processes within a complex system. A more detailed description of the MV-EOF analysis can be found in Wang (1992). In this section, the MV-EOF analysis is adopted to derive useful information about the spatial structure of the coupled ENSO mode in its developmental and mature phases.

a. Mature phase

The most significant EOF (E1) accounts for 40% of the total varianc. The corresponding principal component of E1, $C_1(t)$, is best negatively correlated with the SO index. The simultaneous correlation coefficient is 0.95. Thus the spatial pattern of E_1 represents the extreme phase of an ENSO cycle. The $C_1(t)$ reaches, respectively, a maximum during the mature phase of the five warm episodes (Nov. 1972, Nov. 1976, Dec. 1982, May 1987, and February 1992) and a minimum during the mature phase of the four La Ninas (Feb. 1971, Dec. 1973, Oct. 1975, and Dec. 1988) (Fig. 4d). Note that the mature phases of both E1 Nino and La Nina prefer occurring in boreal late fall and winter (8/9).

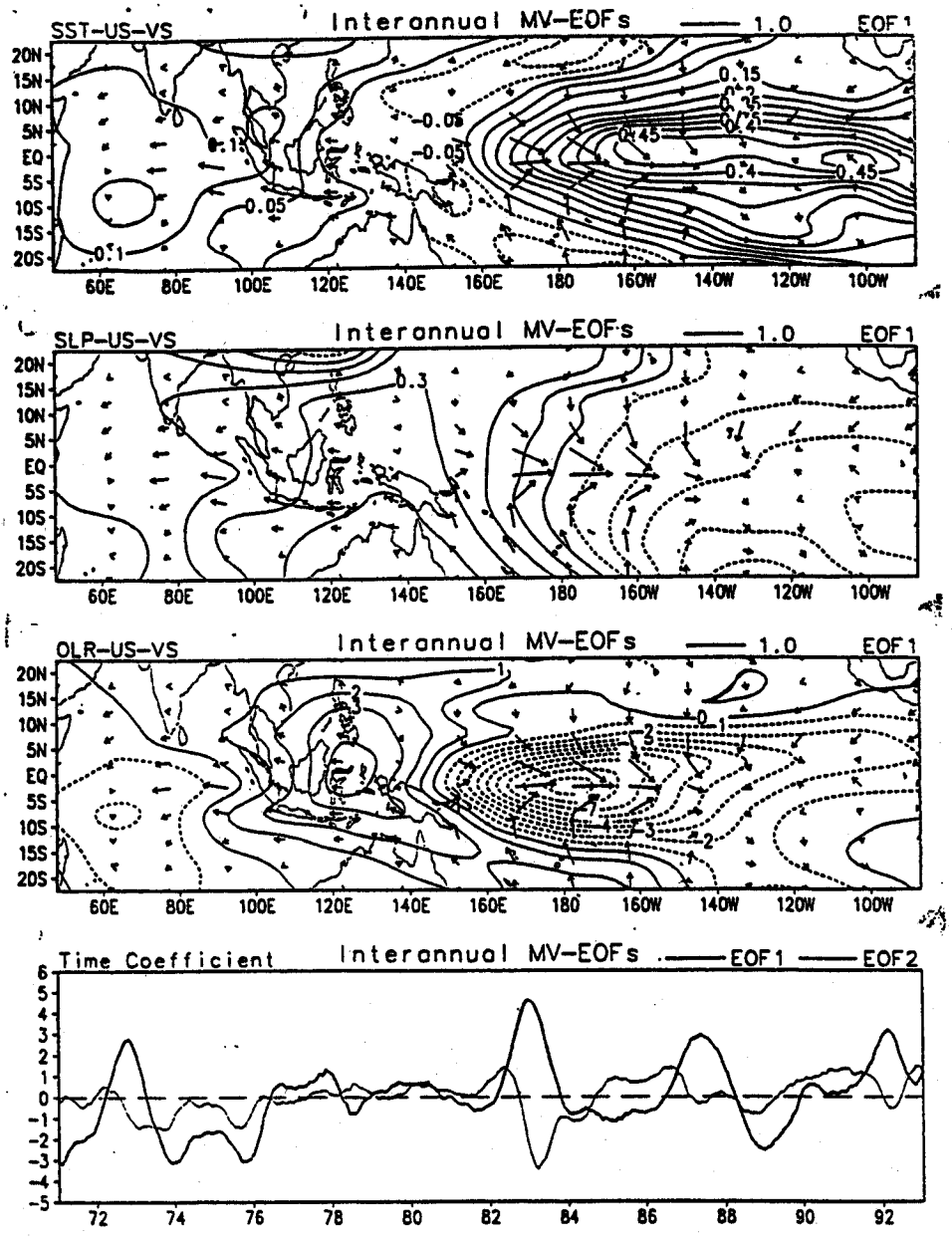

Fig. 4 The spatial patterns of (a) SST and winds, (b) SLP and winds, and (c) OLR and winds of the first multi—variate EOF mode of the seven—month running mean anomalies and (d) the corresponding principal component, $C_1(t)$ (bold).

The mature phase of the El Nino (El mode) exhibits a basin-wide warming with the strongest anomalous warming near 150°W and 110°W at the equator (Fig. 4a). The warming is symmetric about the equator and is accompanied by a weak

cooling in the western Pacific. The cooling area has a U-shape and embraces the warming areas. A slight warming occurs over the tropical Indian Ocean. In association with the warming, SLP falls east of the dateline and rises west of the dateline (Fig. 4b). The anomalous pressure field also exhibits an appreciable asymmetric component with regard to the equator. A larger amplitude occurred in the Southern Hemisphere. Consistent with strong east-west anomalous pressure gradients, remarkable equatorial westerly anomalies prevail from 160°E to 150°W. Prominent equatorward meridional winds are connected with the equatorial westerly anomalies. The surface wind convergence is primarily due to the meridional wind component, indicating the importance of the beta-effect on the equatorial boundary layer flows (Lindzen and Nigam 1987). As a result of the boundary layer convergence, negative OLR anomalies (enhanced convection) tend to be in phase with the equatorial westerly anomalies and located to the west of the highest SST anomalies Fig. 4c). It is noticed that equatorward wind anomalies occur over the intertropical convergence zone (ITCZ) and South Pacific convergence zone (SPCZ), implying an equatorward shift of these convergence zones during the peak phase of the ENSO warming.

Early Warming phase

We note that the principal component of E_2, $C_2(t)$, leads the El mode by about eight months with a lag correlation coefficient of 0.50 which is well above the 99% confidence level (Fig. 5d). This implies that the spatial pattern of E_2 can be viewed as an early phase that precedes the peak warming by about three seasons. The fact that the amplitude of C_1E_1 is about three times as large as that of C_2E_2 indicates an obvlous development of warm events. E_2 thus describes early development characteristics of an ENSO warming.

E2, which accounts for about 12% of the total variance, shows a moderate warming in an elongated zone from the western equatorial Pacific (centered at the equator and 165°E) to subtropical eastern North Pacific (centered at 15°N and 120°W) with a moderate cooling in the eastern Pacific centered at the Ecuador coast (Fig. 5a). The anomalous SLP is strongly asymmetric about the equator. An anomalous low is centered at (20°N, 140°W) with an ENE-WSW oriented trough from the low pressure center to the Philippine Sea (Fig. 5b). The low pressure anomalies are located just northwest of the warming areas along the anomalous SST front in the North Pacific subtropics. Associated with the anomalous pressure trough, an elongated cyclonic gyre is nearly in geostrophic balance with the anomalous low pressure trough (Fig. 5b). Strong westerly anomalies south of the trough tend into the western equatorial pacific. This is the most fundamental factor for

an ENSO warming development. In the eastern Pacific, anomalous winds diverge from an anomalous high generated by the anomalously cold water. It is important to notice that, in accord with the asymmetric anomalous SLP, there are significant cross equatorial winds from the Southern to the Northern Hemisphere, implying an enhanced northern summer-type of Hadley circulation. Because the peak of the E2 mode normally occurs in boreal spring, the implication is that during an El Nino year there is an expedited northern summer circulation. The convection is enhanced over the western Pacific centered at (5°N, 160°E) (Fig. 5c). The regions of enhanced convection nearly coincide with westerly anomalies and are associated with the surface wind convergence which is induced by the meridional wind component. The enhanced and suppressed convection is located to the west of the anomalously warm and cold ocean surface, respectively. The described structure is dynamically consistent, indicating a physical coupling, not a mere statistically deduced pattern.

Another interesting observation is that El has a dominant 5-year period while E2 displays a significant quasi-biennial component. This is consistent with the wavelet analysis in section 3. It suggests a link between the quasi-biennial and quasi-five years oscillation in the ENSO cycle.

5. Summary

The wavelet analysis presented in section 3 reveals that the broad-band period (2-7 years) of the ENSO cycle is attributed to its variability and coexistence of inherent multi-time scales. The period of the ENSO cycle exhibits pronounced interdecadal variations in the last four decades. Around 1964 there was an abrupt shortening of the dominant oscillation period from 6 years to about 2 years. From the middle 1960s to the middle 1970s, the period of the ENSO cycle increased gradually from 2 years to 4-5 years, and in the last two decades or so the ENSO cycle has exhibited a quite regular quasi-5 year oscillation.

The multi-variate EOF analysis was applied to reveal the common characteristics of the ENSO development in the last two decades. It is found that the establishment of an anomalous cyclonic gyre over the Philippine Sea and the westerly anomalies in the western equatorial Pacific are fundamental features of the early development for recent El Ninos. The westerly anomalies are reinforced by the enhanced convection over the western Pacific. Another interesting feature is the enhancement of the southeast trades in the eastern Pacific which apparently delayed the warming in the eastern Pacific so that the Central Pacific warming leads the South American coastal warming in the latest three El Ninos.

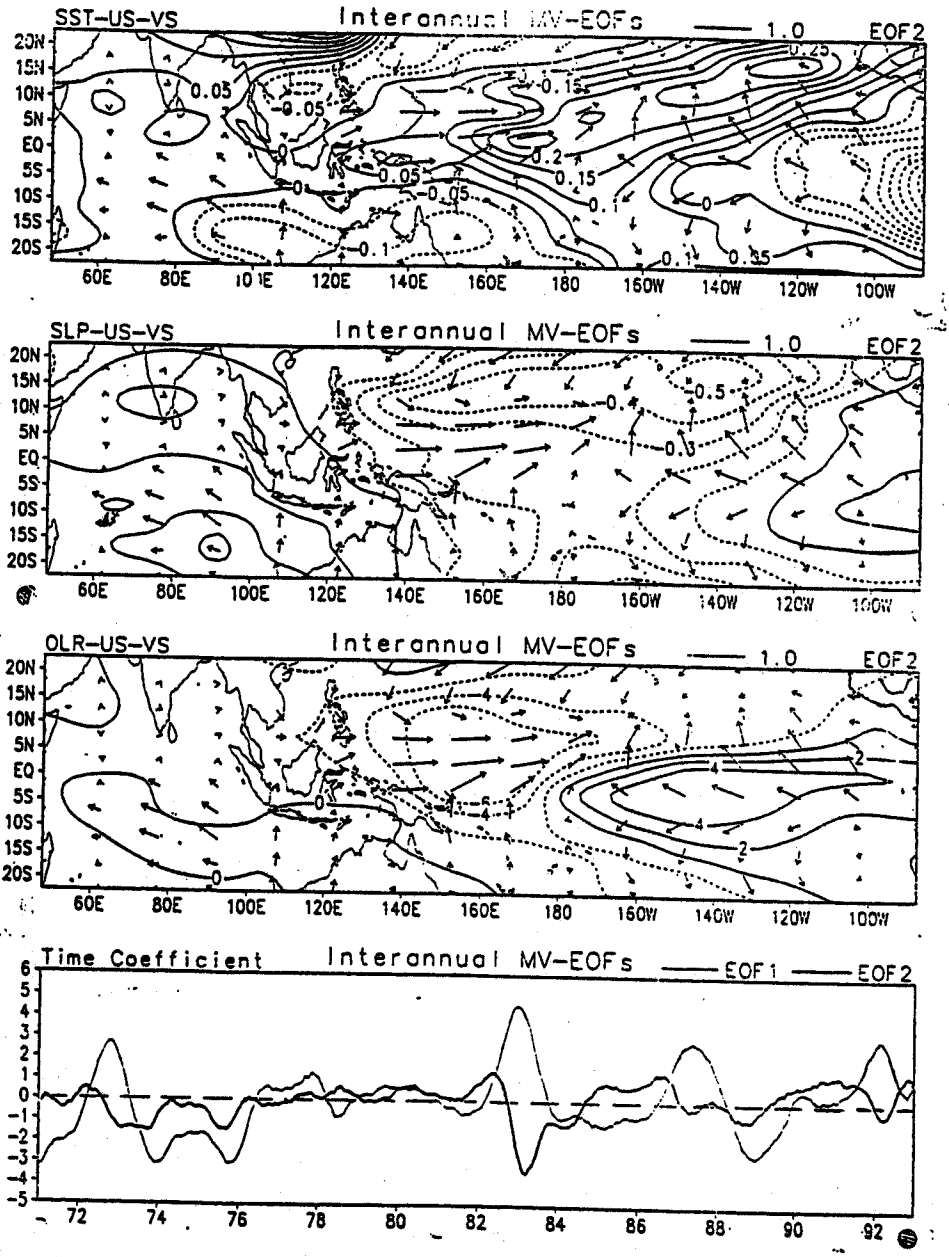

Fig. 5 Same as in Fig. 4 except for the second most significant multi-variate EOF mode

This is the first of a series of papers that are devoted to addressing the nature of the ENSO cycle and the physical causes of the transition from a cold to a warm state of the ENSO cycle. In an accompanying paper (Wang 1994b) the interdecadal changes in the characteristics of the ENSO onset are presented in detail. It is hypothesized that the changes in the ENSO onset after the mid-1970s

are attributed to the changes in the background circulation on which ENSO warming develops. The latter is regulated by a global interdecadal mode. In another forthcoming paper (Wang 1994c) the common characteristics of ENSO onset and development in the last four decades are documented. The sustained eastward anomalous wind stress in the western-central Pacific is believed to be a key element for ENSO development. The amplification and slow eastward propagation of the equatorial westerly anomalies from the western to the central Pacific are hypothesized to result from the effects of zonal variations of the mean winds and the interaction between SST gradients and equatorial zonal winds.

ACKNOWLEDGMENTS

The authors wish to thank Dr. Daifang Gu and Dr. Hengyi Weng for their discussion of wavelet analysis and for kindly providing their numerical codes, We also thank Dr. Julian Wang for sharing his data, and C. Wan and D. Kessler for their technical assistance. This research has been supported by NOAA Equatorial Pacific Ocean Climate Study (EPOCS) program.

References

Barnett, T.P., 1981: Statistical relations between ocean/atmosphere fluctuations in the tropical Pacific. *J.Phys. Oceanogr., 11*, 1043-1058.

1984: Interaction of the monsoon and Pacific trade wind system at interannual time scales. Part Ⅱ: A partial Anatomy of the Southern Oscillation. *Mon.Wea. Rev., 112*, 2388-2400.

Bjerknes, J., 1966: A possible response of the atmospheric Hadley circulation to equatorial anomalies of ocean temperature. *Tellus*, 18, 820-829.

—— 1969: Atmospheric teleconnections from the equatorial Pacific. *Mon. Wea. Rev., 97*, 163-172.

Cane, A.M., 1993: Tropical Pacific ENSO models: ENSO as a mode of the coupled system. In *Climate System Modelings*, Ed. K. E. Trenberth, Cambridge University Press, New York PP788.

Farge, M. 1992: Wavelet transforms and their applications to turbulence. *Ann. Rev. of Fluid Mech., 24*, 395-457.

Garcia, O. S., 1985: Atlas of highly reflective clouds for the global tropics: 1971-1983. U. S. Dept. of Commerce, National Oceanic and Atmospheric Administration, ERL, December 1985.

Gill, A. E., and E. M. Rasmusson, 1983: The 1982-83 climate anomaly in the equ-

atorial Pacific. *Nature*, 306, 229-234.

Goupillaud, P., A. Grossman, and J. Morlet, 1984: Cycle-octave and related transforms in seismic signal analysis. *Geoexploration*, *23*, 85-105.

Gruber, A., and A. F. Krueger, 1984: The status of the NOAA outgoing longwave radiation data set. *Bull. Amer. Met. Soc.*, *65*, 958-962.

Horel, J. D., and J. M. Wallace, 1981: Planetary-scale atmospheric phenomena associated with the Southern Oscillation. *Mon. Wea. Rev.*, *109*, 813-829.

Janowiak, J. E., 1993: Seasonal climate summary: The global climate for September-November 1991: Warm (ENSO) episode condition strengthen. *J.Climate*, *6*, 1616-1638.

Kousky, V. E., 1993: Seasonal climate summary: The global climate for December 1991- February 1992: Mature phase warm (ENSO) episode conditions develop. J. Climate, 6, 1639-1655.

—— *V.E.*, and A. Leetmaa, 1989: The 1986-87 Pacific warm episode: Evolution of oceanic and atmospheric anomaly fields. *J. Climate*, *2*, 254-267.

Lindzen, R.S.,and S. Nigam. 1987: On the role of sea surface temperature gradients in forcing low-level winds and convergence in the tropics. *J. Atmos. Sci.*, *45*,24402458.

Meehl, G. A., 1987: The annual cycle and interannual variability in the tropical Pacific and Indian ocean region. *Mon. Wea. Rev.*, *115*, 27-50.

Meyer, S. D., B. G. Kelly, and J.J. O'Brien, 1993: An introduction to wavelet analysis in oceanography and meteorology: with application to the dispersion of Yanai waves, *Mon. Wea. Rev.*, in press.

Philander, S. G., 1985: El Nino and La Nina. *J. Atmos. Sci.*, *42*, 2652-2662.

Rasmusson, E. M., and T. H. Carpenter, 1982: Variations in tropical sea surface temperature and surface wind fields associated with the Southern Oscillation/ El Nino. *Mon. Wea. Rev.*, *110*, 354-384.

Trenberth, K. E., 1992: General characteristics of El Nino-Southern Oscillation. In Climate System Modeling, Ed.K.E. Trenberth, Cambridge University Press, New York PP788.

—— and D.J. Shea, 1987: On the evolution of the Southern Oscillation. *Mon. Wea. Rev.*, *115*, 3078-3096.

Van Loon, H. and *D. J. Shea*, 1985: The Southern Oscillation. Part Ⅳ: The precursors south of 15°S to the extremes of the oscillation *Mon. Wea. Rev.*, *113*, 20632074.

—— and —— 1987: The southern Oscillation. Part Ⅵ: Anomalies of sea level pressure on the southern Hemisphere and of Pacific sea surface temperature during the development of warm Event. *Mon. Wea. Rev.*, *115*, 370-379.

Wallace, J.M. and D.S. Gutzler, 1981: Teleconnections in the geopotential height during the Northern Hemisphere winter. *Mon. Wea. Rev.*, *109*, 784-812.

Wang, B., 1992: The vertical structure and development of the ENSO anomaly mode during 1979-1989. *J. Atmos.Sci.*, *49*, 698-712.

—— 1994a: On the annual cycle in the tropical eastern-central Pacific. *J. Climate*. In press.

—— 1994b: Interdecadal changes in El Nino onset in the last four decades. *J. Climate*. In press.

—— 1994c: Transition from a cold to a warm state of the El Nino-Southern Oscillation cycle. *Meteor. Atmos. Physics*. In press.

Wyrtki, K., 1975: El Nino-the dynamic response of the equatorial Pacific Ocean to atmospheric forcing. *J. Phys. Oceanogr.*, *5*, 572-584.

1971—1992年期间埃尔尼诺的发展期特征

王 煜 王 炎

（夏威夷大学 海洋与地球科技学院 气象系）

摘 要

小波(wavelet)分析的结果表明埃尔尼诺—南方涛动(ENSO)循环的周期从本世纪五十年代以来经历了显著的变化。其主周期在六十年代中期由六年左右突变为二年左右，随后逐渐增为4年左右。七十年代中期之后，ENSO循环呈现准5年振荡，同时也含有一个明显的准两年振荡分量。

最近二十年来，ENSO循环中由冷到暖的状态转换过程有值得注意的相似性。对1971—1992年间的海温、海表气压和风场以及深对流场所做的多变量经验正交函数(MV—EOF)分析指出，最重要的模态描述暖事件的成熟期，第二模态描述暖事件的发展期。ENSO发展期具有以下主要特征：1)在整个热带北太平洋上空有一个准东西向的异常低气压带；2)与此异常低压相适应，在西北热带太平洋出现异常气旋环流，在赤道西太平洋出现异常强西风，在赤道东、中太平洋的越赤道东南信风加强；3)深对流异常区与西太平洋异常西风区几乎重合，它主要是由异常的经向风向赤道的辐合所致。描述发展期的第二模态表现出明显的准两年分量。这与描述成熟期的以5年为主周期的第一模态形成鲜明的对比。

关键词：埃尔尼诺—南方涛动(ENSO)，多变量经验正交函数(MV—EOF)